Science
AAAS

Formation of Catalytic Metal-Molecule Contacts
George S. Tulevski, *et al.*
Science **309**, 591 (2005);
DOI: 10.1126/science.1112767

Science (print ISSN 0036-8075; online ISSN 1095-9203) is published weekly, except the last week in December, by the American Association for the Advancement of Science, 1200 New York Avenue NW, Washington, DC 20005.

Formation of Catalytic Metal-Molecule Contacts

George S. Tulevski,[1] Matt B. Myers,[1] Mark S. Hybertsen,[2] Michael L. Steigerwald,[1]* Colin Nuckolls[1]*

We describe a new strategy for the in situ growth of molecular wires predicated on the synthesis of a trifunctional "primed" contact formed from metal-carbon multiple bonds. The ruthenium-carbon π bond provides structural stability to the molecular linkages under ambient conditions, and density functional calculations indicate the formation of an efficient conduit for charge carriers to pass between the metal and the molecule. Moreover, the metal-carbon π bond provides a chemically reactive site from which a conjugated molecular wire can be grown in situ through an olefin metathesis reaction.

For single-molecule electronics, more effort has been invested in the design and synthesis of the molecules and less in the fabrication of the molecule-to-metal contact. A common approach for molecular wires is an extended, conjugated, organic π system bonded to a metal surface (most frequently as a thiol linkage to gold) (*1*). One limitation is that the gold thiol linkage is only structural; it lacks any subsequent chemistry that is useful. Also, because it is difficult to modify the energies and occupations of the sulfur 3*p* orbitals substantially, the metal-thiolate contact lacks an essential orbital conduit for electrons and/or holes.

We present an alternative strategy for the in situ growth of molecular wires predicated on the synthesis of a trifunctional "primed" contact formed from metal-carbon multiple bonds. The primed contact provides static structural stability and a chemically reactive site from which a molecular wire can be grown. It should also create an efficient conduit for charge carriers to pass between the metal and the molecule; the metal-carbon π bond continues the π conjugation from the conjugated molecule directly into the metal. The metal-carbon π bond is active in the olefin metathesis reaction, indicating that the reactivity of such sites can be exploited to grow conjugated molecular wires in situ.

Ruthenium (Ru) is an attractive material for electrodes because it readily forms hard, highly conductive thin films (*2*). It is also a very active catalytic metal; carbene complexes in solution can catalyze the metathesis of olefins (*3*). There are precedents for Ru-surface carbene complexes in ultrahigh vacuum (UHV): one using diazomethane (*4*) and the other diphenyl diazomethane (*5*). In addition, the UHV studies of McBreen and co-workers have shown that surface molecule multiple bonds on metal-carbide surfaces are some of the most thermally stable adlayers (*6*) and are catalytically active (*6*–*8*). We found that a freshly prepared Ru thin film (*9*) reacts at room temperature with either 4-bromophenyldiazomethane (**1**) or trimethylsilyldiazomethane (**2**) to give the derivatized surfaces **1a** and **2a**, respectively (insets to Figs. 1 and 2) (*10*). In each case, the C-N bond cleaves, and the C(H)R (R = 4-bromophenyl or trimethylsilyl, respectively) fragment bonds directly to the metal. Scanning tunneling microscopy images on ruthenium single crystals indicate that a single, dense layer forms (*11*).

The photoelastic modulation infrared (IR) reflection-absorption spectrum (*12*) of **1a** (Fig. 1A) contains the C=C symmetric stretching modes at 1610 and 1585 cm^{-1} characteristic of a 1,4-disubstituted phenyl group. Three other major resonances are also present: the C=C asymmetric stretch (1465 cm^{-1}) and the parallel (1370 cm^{-1}) and perpendicular (940 cm^{-1}) in-plane ring stretches (*13*, *14*). We did not observe any stretching modes indicative of the dibromostilbene that would result from the coupling of two carbenes or from a diazo functionality. The x-ray photoelectron spectrum (XPS) (*12*) of **1a** shows the presence of the characteristic Br doublet arising from the $3d_{5/2}$ and $3d_{3/2}$ core levels (*15*, *16*).

For the reaction between a freshly prepared Ru surface and trimethylsilyldiazomethane, **2**, the IR spectrum is dominated by two sets of peaks: one a broad and intense resonance at around 1200 cm^{-1} and the other a cluster of three peaks (2953, 2916, and 2854 cm^{-1}) (fig. S1A) (*12*). The former is well known in methylsilane monolayers (*17*) and arises from the silicon-carbon stretch of the trimethylsilyl (TMS) group. The other three peaks are the asymmetric (2953 cm^{-1}) and symmetric (2916 and 2854 cm^{-1}) stretches indicative of terminal methyl groups (*17*). Again, there was no evidence of a diazo stretch or an alkene stretch. The XPS for **2a** shows the expected transition at about 100.5 eV for the silicon 2*p* core levels

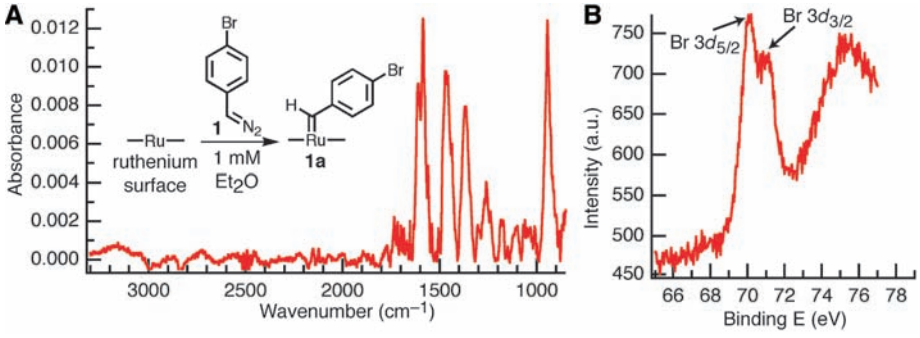

Fig. 1. To form the monolayer **1a**, a fresh ruthenium surface reacted with 4-bromophenyldiazomethane (**1**). (**A**) Surface polarized IR spectrum. (Inset) Reaction of a ruthenium surface with 4-bromophenyldiazomethane to give a derivatized surface. (**B**) XPS showing the presence of bromine atoms. a.u., arbitrary units.

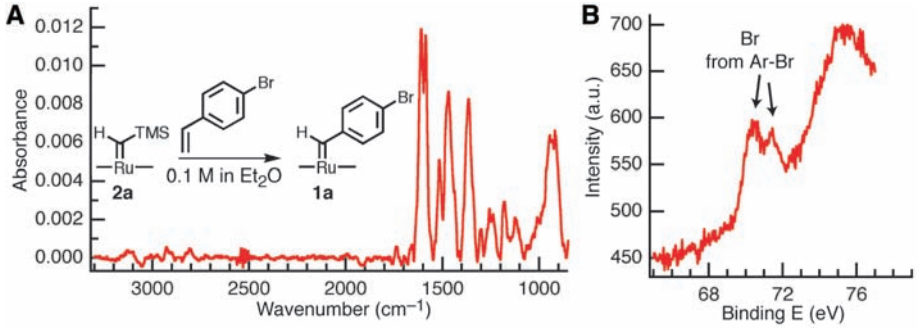

Fig. 2. Conversion of **2a** into **1a** with the use of a 1 mM solution of 4-bromostyrene in ether. (**A**) IR spectrum. (Inset) Reaction of derivatized surface **2a** with 4-bromostyrene to give derivatized surface **1a**. (**B**) XPS from the bromine after reaction. a.u., arbitrary units.

[1]Department of Chemistry and the Nanoscience Center, [2]Department of Applied Physics and Applied Mathematics and the Nanoscience Center, Columbia University, New York, NY 10027, USA.

*To whom correspondence should be addressed. E-mail: cn37@columbia.edu (C.N.); mls2064@columbia.edu (M.L.S.)

from the TMS group (fig. S1B) (*18*). The only other diagnostic feature in the XPS spectra from either **1a** or **2a** is the presence of well-known ruthenium nitrides (*19*–*21*).

These monolayers on Ru are exceedingly stable. We took no measures to protect the samples from oxygen or moisture, yet the XPS and IR signals from the monolayers remained unchanged when measured intermittently over the course of a few days. When we heated the films to 160°C for several hours the only detectable difference in the spectra was the conversion of the molecular nitride into the atomic nitride—a well-studied process (fig. S2) (*20*, *21*). Similarly, when the monolayers were placed into solvents such as ether, tetrahydrofuran (THF), or dodecane overnight they showed no change.

The IR and XPS data show that diazoalkanes react with a Ru surface, but it is yet to be determined the exact nature of the bonding of the otherwise divalent carbon to the surface of the metal. This C atom may form the carbon-metal double bond to a single surface Ru atom, as deduced from previous UHV studies (*4*, *5*). A second alternative is that the carbon bridges adjacent surface atoms, in either a doubly or triply bridge bonded arrangement. Unfortunately, we cannot observe spectral features assignable to any of these modes, and therefore we cannot distinguish which bonding form occurs in the present samples.

The distinction between the bonding modes may not be as practically important as one might imagine. Even if the carbene carbon bonds in a bridging fashion to two or more Ru atoms, its chemical reactivity should be similar to that of a "mononuclear" metal carbene. In solution, they show qualitatively similar chemistry when the carbene is either bridge-bonded between two ruthenium atoms or when there is an unambiguous carbon-ruthenium double bond (*22*) (although the former is catalytically less active).

In any case, we found that the surface-bound $Ru_nC(H)(R)$ unit can catalyze olefin metathesis and that the Ru-C linkage behaves sufficiently like a multiple bond that it warrants further study as a molecule-to-metal contact. When we treated **2a** (prepared from **2** as above) with a large excess of 4-bromostyrene in diethylether overnight at room temperature, we saw the spectral features characteristic of **2a** disappear and those of **1a** appear (Fig. 2) (*23*). After reaction, the characteristic XPS signature for Br was present (Fig. 2B), but the Si signature from the TMS group at ~100.5 eV was absent (fig. S3). Similarly, the IR spectrum shows the loss of the intense C-Si stretch and appearance of the four resonances characteristic of the parasubstituted phenyl ring of **1a**. The spectra of the surfaces prepared by means of diazoalkanes and by means of metathesis show different ratios of the C-C ring-stretching doublet around 1600 cm^{-1}, an indication of the surface conformation of parasubstituted aromatics, that likely reflects the different density of carbenes on the two surfaces.

The converse reaction, converting monolayer **1a** into a monolayer **2a** using vinyltrimethylsilane (Fig. 3A) also occurs. Under identical conditions to those used above for **2a**, the conversion to **1a** gives a mixture of different carbenes on the surface in approximately 8:5 ratio indicating a 60% conversion (fig. S4). This reaction does not proceed to completion, whereas the reverse reaction does. This difference could be due to the surface **1a** (prepared from **1**) having a higher density of carbenes compared with that of surface **2a** (prepared from **2**) based on the larger cross-sectional area for the bulky trimethylsilyl group, so that it is not possible to fully convert **1a** to **2a** by metathesis.

The data in Fig. 3B obtained with gas chromatography/mass spectrometry (GC/MS) serve as a strong indication that the surface reaction proceeds through a metathesis reaction. To aid in the analysis (by increasing the surface area and therefore the amount of the 4-bromostyrene produced), ruthenium particles were used instead of planar metal films. These Ru particles were allowed to react with **1** and then placed in a solution of vinyltrimethylsilane. Both a 4-bromostyrene standard and the reaction mixture showed a peak in the chromatogram at a retention time of 7.27 min. The mass spectrum of this peak in both cases shows the expected mass and isotope pattern from 4-bromostyrene. The demonstration of a surface-initiated olefin metathesis reaction not only provides evidence of the multiple bond character of the Ru-C link but is also essential to our broader strategy of in situ synthesis of molecular wires starting from a primed metal surface (Fig. 3C).

A carbene precursor such as a diazoalkane is necessary to initiate any of this chemistry. For example, when a fresh Ru surface is treated with either 4-bromostyrene or vinyltrimethylsilane under the conditions that led to metathesis (above), we did not observe bromine or silicon peaks in the XPS. Also, a "carbene metal" such as Ru is necessary; the use of Au instead of Ru in these reactions did not produce a derivatized Au surface. Neither of the diagnostic peaks that result from the reaction of **2** with Ru (i.e., the Si-C stretch at 1236 cm^{-1} nor the Si peak in the XPS at 100.5 eV) was present when we treated a Au film with a solution of **2** in ether (fig. S5).

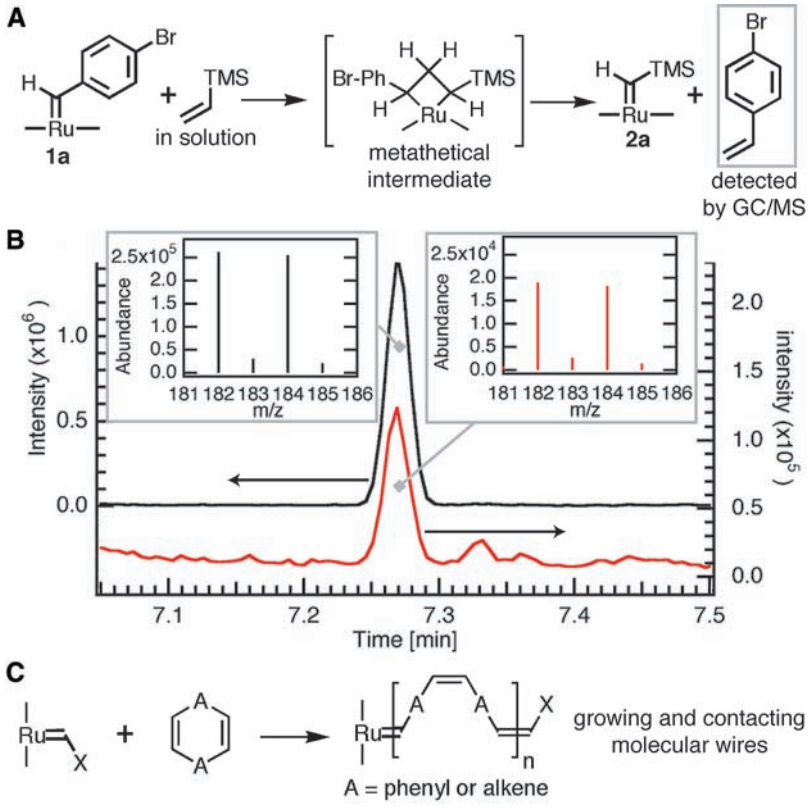

Fig. 3. (**A**) Reaction of **1a** with vinyl-trimethylsilane through a surface metathesis reaction to yield **2a** and 4-bromostyrene. (**B**) The 4-bromostyrene can be detected by GC/MS. The insets show the characteristic mass and isotope pattern for the 4-bromostyrene standard (left inset) and for the reaction mixture (right inset). m/z, mass-to-charge ratio. (**C**) Ring opening metathesis polymerization pathway to conjugated molecular wires in electrical contact with a Ru metal particle or surface.

To understand the bonding of the ruthenium surface carbenes and the character of the electronic states that link to a molecular wire, we conducted a series of density functional theory calculations (*24*, *25*). Both Ru clusters (*26*) and periodic slabs (*27*, *28*) of Ru have been considered, coupled to several different carbenes. In Fig. 4A, we show results obtained for a carbene at the end of a 1,3-pentadienchain, C_5H_6: The conjugated π system forms a short molecular "wire," whereas the terminal divalent carbon forms the carbene link to the metal. The bonding to the atop site on the Ru(0001) surface with the terminal carbene forms a simple double bond, giving a Ru-C bond length of 1.96 Å. The length of the adjacent C-C single bond is similar to that of the corresponding bond in the related hexa-1,3,5-triene (table S1). Figure 4A also shows the frontier π orbital for the RuC_5H_6 molecule. The Ru-to-C π bonding is essentially continuous with the rest of the π system on the molecule. Figure 4B shows the parallel comparison for C_5H_5, a carbyne, bonded in the hexagonally close-packed hollow site of the Ru(0001) surface. Again, the continuity of the π system bonding on the molecule is apparent and the geometry of the C_5H_5 is indistinguishable from the double-bonded organic analog.

The degree of coupling of the π system to the extended states in the metal was monitored by computing the local density of states as a function of energy, projecting on the region of the last two C atoms in the molecule. The results are shown for energies near the Ru metal Fermi energy in Fig. 4C (*29*). The occupied resonance clearly has the character of the highest occupied π state in the organic, with two nodes along the chain. The unoccupied resonance is similarly derived from the first empty π state, with three nodes along the chain (including the link to the surface.) The occupied resonance is quite broad, and the state has the general character of the organic π state throughout. These results indicate that the π bonding on the organic backbone couples smoothly to the *d* orbitals in the Ru metal. This looks very promising as a high conductance link between the Ru metal and the molecule. The π resonance overlaps the metal Fermi energy and is partially empty. This is consistent with the calculated change in the work function upon formation of this 2×2 adlayer (namely ~–0.5 eV).

This study demonstrates that solution-phase chemistry can be used to form stable monolayers between carbenes and ruthenium surfaces. These surface-bound carbenes are able to initiate olefin metathesis. Given the strong electronic coupling between the molecular π states and the conducting states in the metal, these systems form primed contacts with utility in molecular electronics as highly conductive and catalytic sites for in situ wire growth from electrode surfaces.

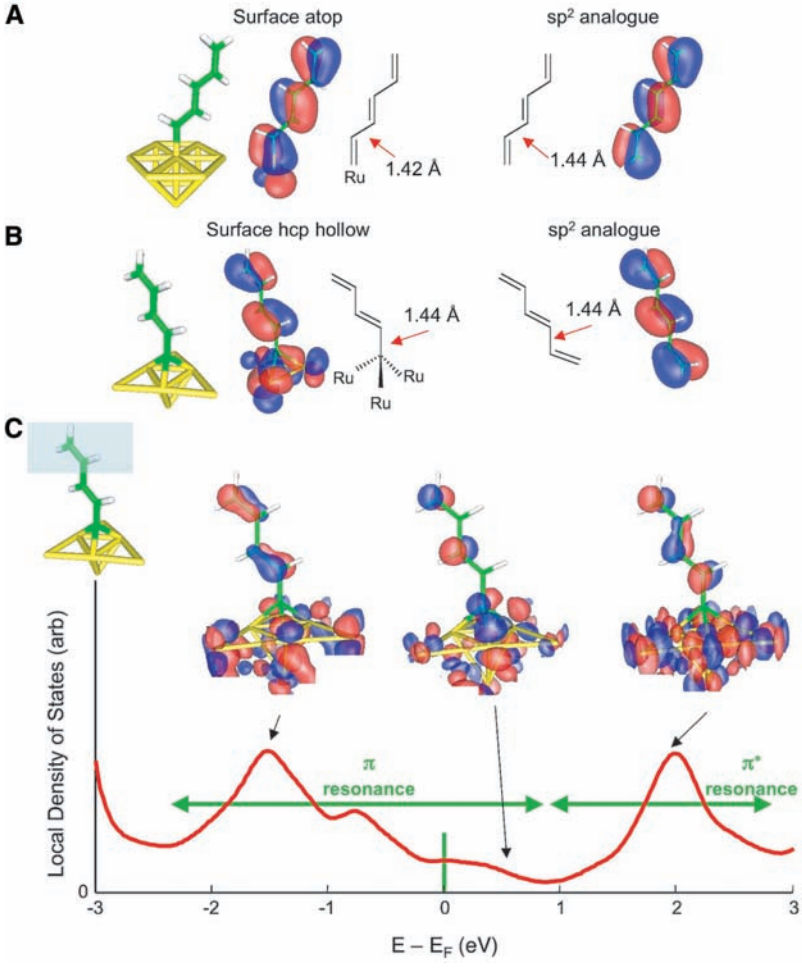

Fig. 4. Two candidate bonding geometries. (**A**) Atop binding of a carbene on the Ru(0001) surface and (**B**) threefold hexagonal close-packed (hcp) hollow site binding of the carbyne on the Ru(0001) surface. Results for the relaxed geometry computed for the 2×2 surface unit cell are compared to those for a C_6H_8 organic analog. The highest occupied π state for the pentadienyl fragments bound to the ruthenium cluster is compared to the analog in an isosurface plot. (**C**) Local density of states for the carbyne bonded to the hcp hollow of the Ru(0001) surface (modeled by a four monolayer slab) for energies near the Ru Fermi energy. The state density is projected on the region of the last two carbon atoms on the chain as indicated. Isosurface plots for selected wave functions are shown. The plots are truncated to the near-surface region. arb, arbitrary units.

References and Notes

1. A. Nitzan, M. A. Ratner, *Science* **300**, 1384 (2003).
2. H. Zhong, G. Heuss, Y.-S. Suh, V. Misra, S.-N. Hong, *J. Electron. Mater.* **30**, 1493 (2001).
3. R. H. Grubbs, *The Handbook of Olefin Metathesis,* R. H. Grubbs, Ed. (Wiley-VCH, Weinheim, ed. 1, 2003).
4. P. M. George, N. R. Avery, W. H. Weinberg, F. N. Tebbe, *J. Am. Chem. Soc.* **105**, 1393 (1983).
5. M. Gunia, P. Jakob, W. Sander, C. Woell, *J. Phys. Chem. B* **108**, 14025 (2004).
6. E. M. Zahidi, H. Oudghiri-Hassani, P. H. McBreen, *Nature* **409**, 1023 (2001).
7. M. Siaj, C. Reed, S. T. Oyama, S. L. Scott, P. H. McBreen, *J. Am. Chem. Soc.* **126**, 9514 (2004).
8. M. Siaj, H. Oudghiri Hassani, E. Zahidi, P. H. McBreen, *Surf. Sci.* **579**, 1 (2005).
9. To form the monolayers **1a** and **2a**: 200 nm of Ru metal (Kurt J. Lesker) was sputtered onto silicon wafers (Silicon Sense) with the use of a home-built sputtering chamber. The native oxide was removed from the samples by hydrogenation (1 atm H_2, 120°C, 1 hour) immediately before use. The metal films were immersed in a solution of either **1** (0.1 mM solution in benzene) or **2** (0.1 mM solution in Et_2O) for 2 hours, and then they were removed, rinsed in copious amounts of fresh solvent, and dried under a stream of nitrogen gas.
10. D. S. Wulfman, S. Yousefian, J. M. White, *Synth. Commun.* **18**, 2349 (1988).
11. G. Flynn, M. Lay, G. S. Tulevski, M. L. Steigerwald, C. Nuckolls, data not shown.
12. Materials and methods are available as supporting material on *Science* Online.
13. Here, parallel and perpendicular refer to the 1,4-phenyl axis.
14. R. Arnold, A. Terfort, C. Woell, *Langmuir* **17**, 4980 (2001).
15. We used **1** and **2** in these studies because they carry marker atoms (i.e., bromine or silicon) that are easily identified with XPS. These marker atoms are necessary because the carbon 1*s* core level cannot be monitored because its x-ray photoelectron energy is coincident with the ruthenium $3d_{5/2}$ core level.
16. Y. Kaga, Y. Abe, H. Yanagisawa, M. Kawamura, K. Sasaki, *Surf. Sci. Spectra* **6**, 68 (1999).
17. J. R. Combes, L. D. White, C. P. Tripp, *Langmuir* **15**, 7870 (1999).
18. S. R. Wasserman, Y. T. Tao, G. M. Whitesides, *Langmuir* **5**, 1074 (1989).
19. T. Birchem, M. Muhler, *Surf. Sci.* **334**, L701 (1995).
20. K. Jacobi, *Phys. Status Solidi A* **177**, 37 (2000).
21. E. Umbach, *Solid State Commun.* **51**, 365 (1984).
22. M. R. Gagne, R. H. Grubbs, J. Feldman, J. W. Ziller, *Organometallics* **11**, 3933 (1992).

23. Conditions for metathesis reaction: **1a** or **2a**, prepared from the corresponding diazoalkanes, was immersed in a solution (0.1 M solution in THF) of the corresponding alkenes for 2 hours. The films were removed, rinsed with fresh THF, and dried under a stream of nitrogen gas.
24. The generalized gradient approximation was used (*12*, *25*).
25. J. P. Perdew, K. Burke, M. Ernzerhof, *Phys. Rev. Lett.* **77**, 3865 (1996).
26. Jaguar 5.0, Schrodinger, L.L.C., Portland, OR (1991–2003).
27. The ABINIT code is a common project of the Université Catholique de Louvain, Corning Incorporated, and other contributors (www.abinit.org).
28. X. Gonze *et al.*, *Comp. Mater. Sci.* **25**, 478 (2002).
29. The substructure of the occupied resonance is due to the size of the slab (4 monolayers). However, there is continuous state density through this energy region, resulting from dispersion of the states in the direction parallel to the surface.
30. We acknowledge primary financial support from the Nanoscale Science and Engineering Initiative of the NSF under NSF award number CHE-0117752 and by the New York State Office of Science, Technology, and Academic Research (NYSTAR). We acknowledge support from the Chemical Sciences, Geosciences and Biosciences Division, Office of Basic Energy Sciences, U.S. Department of Energy (#DE-FG02-01ER15264). C.N. thanks the American Chemical Society Petroleum Research Fund type G (#39263-G7), the Camille Dreyfus Teacher Scholar Program (2004), and the Alfred P. Sloan Fellowship Program (2004). We thank the Materials Research Science and Engineering Center Program of the NSF under award number DMR-0213574 and by the NYSTAR for financial support for M.L.S. and the shared instrument facility.

Supporting Online Material
www.sciencemag.org/cgi/content/full/309/5734/591/DC1
Materials and Methods
Figs. S1 to S5
Table S1
References

25 March 2005; accepted 10 June 2005
10.1126/science.1112767

Martian Surface Paleotemperatures from Thermochronology of Meteorites

David L. Shuster[1]* and Benjamin P. Weiss[2]†

The temporal evolution of past martian surface temperatures is poorly known. We used thermochronology and published noble gas and petrographic data to constrain the temperature histories of the nakhlites and martian meteorite ALH84001. We found that the nakhlites have not been heated to more than 350°C since they formed. Our calculations also suggest that for most of the past 4 billion years, ambient near-surface temperatures on Mars are unlikely to have been much higher than the present cold (<0°C) state.

Daily mean equatorial temperatures on Mars are close to 215 K. Surface geomorphic evidence of the flow of liquids, weathering minerals indicative of liquid/rock interactions, and the enrichment of heavy isotopes of several atmospheric species have led to suggestions that early Mars was significantly warmer, with temperatures possibly remaining above 273 K for extended periods of time (*1*). On the basis of crater counting statistics, the colder, drier conditions are thought to have emerged at ~3.7 billion years ago (Ga), with large (~10^8 to 10^9 years) uncertainties (*2*). The growing geochemical and petrographic data set for martian meteorites (*3*) provides an opportunity to constrain the martian paleoclimate using multiple independent samples. We used noble gas thermochronometry of meteorites as an indicator of the evolution of surface temperatures on Mars.

K/Ar and $^{40}Ar/^{39}Ar$ dating studies have been conducted on all seven known nakhlites (*4*) and on martian meteorite ALH84001 (*5*, *6*). Fifteen K/Ar analyses on the nakhlites all give ages of ~1.3 Ga, which are nearly identical to crystallization ages specified by the Rb/Sr, U/Pb, and Sm/Nd chronometers (*7*) and much older than the 11 million years ago (Ma) age of ejection from Mars, as specified by cosmic ray exposure dating (*8*, *9*). (U-Th)/He dating of the nahklites meteorites Nakhla, Lafayette, and MIL03346 (*10*, *11*) has measured similarly ancient (~0.8 to 1.2 Ga) ages. The coincidence of the K/Ar and (U-Th)/He ages with the other chronometers suggests that the nakhlites have experienced no major heating since they formed. Similarly, the ancient 4 Ga $^{40}Ar/^{39}Ar$ age (*6*) and 4 Ga U/Pb apatite age (*12*) for ALH84001 suggests that this meteorite, which has Rb/Sr and Sm/Nd crystallization ages of 4.5 Ga and a cosmic ray exposure age of 15 Ma (*13*), has not experienced any major heating since 4 Ga. This is generally consistent with (U-Th)/He dating of ALH84001 phosphate, which gives a wide range of ages between 0.1 and 3.5 Ga (*14*). Like the nakhlites, the $^{40}Ar/^{39}Ar$ age of Chassigny is ~1.3 Ga and is close to its Sm/Nd and Rb/Sr crystallization ages (*6*, *13*). $^{40}Ar/^{39}Ar$ ages for most shergottites are ambiguous because of significant abundances of trapped Ar (*6*, *13*).

Using whole-rock ^{39}Ar release data of Swindle and Olson (*15*) and following the methods of (*5*, *16*), we estimated the temperature dependence of the Ar diffusion coefficient $D(T)$ through the feldspar in Nakhla and Lafayette, assuming a spherical diffusion domain geometry (*17*). We first considered Swindle and Olson's Nakhla subsample 1. We assumed that the colinearity observed for the first ~80% of the released ^{39}Ar (Fig. 1) indicates that the diffusion of Ar in Nakhla is thermally activated over this range. We also assumed that the presence of distinct arrays clearly separated by breaks in slope (Fig. 1) indicates that multiple diffusion domains are present. From this, we identified three (or possibly even four) primary arrays from the ^{39}Ar data and adopted the interpretation of (*15*) that the first three domains [the low-retentivity domain (LRD) and the one or two high-retentivity domains, which we will refer to as HRD and HHRD] likely represent iddingsite (LRD) and predominantly potassium feldspar admixed with plagioclase (HRD and HHRD). The final array, composed of the final ~20% of gas released, appears to be from a phase (probably clinopyroxene) implanted with recoiled ^{39}Ar (*15*, *18*).

We characterized the spatial distribution of radiogenic ^{40}Ar ($^{40}Ar^*$) and the Ar diffusion kinetics in the HRD alone. The HRD corresponds to the ~1.3 Ga $^{40}Ar/^{39}Ar$ plateau age identified in (*15*). We calculated a diffusion domain model by assuming that the neutron-induced ^{39}Ar distributions were initially uniform within two distinct domains. Gas was not permitted to exchange between the domains. We derived the following diffusion parameters for the two-domain (LRD and HRD only) model for the HRD of Nakhla: activation energy E_a = 117 ± 5.4 kJ mol^{-1} and $\ln(D_o/a^2)$ = 5.7 ± 0.9 $\ln(s^{-1})$ for diffusivity at infinite temperature D_o and diffusive length scale a. These are in good agreement with diffusion parameters estimated for terrestrial potassium feldspars (*19*). Nearly identical results were obtained for the nakhlite Lafayette and another Nakhla subsample (fig. S1, A and B). Similar [within a factor of ~1.2 and ~2.4 for E_a and $\ln(D_o/a^2)$, respectively] values for the HRD were also obtained for a subset one-domain (HRD only) regression (*20*) and a three-domain (LRD, HRD, and HHRD) model, indicating that the inferred diffusion kinetics are not strongly sensitive to the form of the domain modeling (*21*).

In the following calculations, we assume that this Arrhenius relation and corresponding diffusive length scale a have held for the nakhlites' HRD since 1.3 Ga (*22*). The model

[1]Division of Geological and Planetary Sciences, California Institute of Technology, 100-23, Pasadena, CA 91125, USA. [2]Department of Earth, Atmospheric, and Planetary Sciences, Massachusetts Institute of Technology, 54-724, Cambridge, MA 02139, USA.

*Present address: Berkeley Geochronology Center, 2455 Ridge Road, Berkeley, CA 94709, USA
†To whom correspondence should be addressed. E-mail: bpweiss@mit.edu